Supplementary Information

Eco-friendly fabrication of sponge-like magnetically carbonaceous fiber aerogel for high-efficiency oil-water separation

Rui-Lin Liu [a], Xing-Qiang Li [b], Hui-Qin Liu [b], Zhi-Min Luo [a], Jin Ma [c], Zhi-Qi Zhang [c], Qiang Fu [a*]

[a] *School of Pharmacy, Xi'an Jiaotong University, Xi'an 710061, PR China.*

[b] *School of Stomatology, Xi'an Jiaotong University, Xi'an 710061, PR China.*

[c] *School of Chemistry and Chemical Engineering, Shaanxi Normal University, Xi'an 710062, China.*

[*]Corresponding author

Fax: 86-29-82655382; E-mail: fuqiang@mail.xjtu.edu.cn.

Table S1. Comparison of various sorbent materials

Sorbent materials	Absorbed substances	Sorption capacity (g g^{-1})	Cost	Ref.
Wool-based nonwoven	diesel, crude oil, SN 150	9-15	low	[1]
Vegetable fiber	crude oil	1-100	low	[2]
Polymers	oils and organic solvents	5-25	medium	[3]
Nanowire membrane	oils and some organic solvents	4-20	low	[4]
Exfoliated graphite	heavy oil	60-90	low	[5]
Activated carbons	benzene, toluene	<1	low	[6]
Carbon nanotube sponges	oils and organic solvents	80-180	high	[7]
Magnetic exfoliated graphite	oils	30-50	high	[8]
Graphene/a-FeOOH composite	cyclohexane, toluene, vegetable oil, etc.	10-30	high	[9]
Graphene/CNT foam	compressor oil, organic solvents	80-140	high	[10]
Graphene-based sponges	oils and organic solvents	60-160	high	[11]
Carbonaceous nanofiber aerogel	oils and organic solvents	40-115	high	[12]
Graphene sponge	oils and organic solvents	60-160	high	[13]
Reduced graphite oxide foam	cyclohexane, chlorobenzene, toluene, petroleum, motor oil	5-40	high	[14]
Nitrogen doped graphene foam	oils and organic solvents	200-600	high	[15]
Marshmallow-like gels	oils and organic solvents	6-15	high	[16]
CNT sponge doped with boron	oils and organic solvents	25-125	high	[17]
UFAs	oils and organic solvents	215-743	high	[18]
CNF aerogels	oils and organic solvents	106-312	low	[19]
TCF aerogel	oils and organic solvents	50-192	low	[20]
Ultralight magnetic foams	oils and organic solvents	61-102	medium	[21]
3D macroporous Fe/C	oils	4-10	high	[22]
Nanocellulose aerogels	oils and organic solvents	20-40	medium	[23]
Spongy graphene	oils and organic solvents	20-86	high	[24]
Carbon aerogel from winter melon	oils and organic solvents	16-50	low	[25]
MCF aerogel	oils and organic solvents	22-87	quite low	present work

Table S2. Pore volumes of MCF aerogel calculated from the uptake of various organic liquids

	Weight gain (g g^{-1})	Density (g cm^{-3})	Pore volume (cm^3 g^{-1})
Gasoline	28.07	0.73	38.45
Diesel oil	32.57	0.83	39.24
Pump oil	74.63	0.87	85.78
Colza oil	40.86	0.93	43.94
DMSO	46.50	1.10	42.27
Ethanol	27.46	0.79	34.76
PEG-200	86.83	1.27	68.37
Methanol	37.42	0.79	47.37
Phenoxin	69.32	1.6	43.33
THF	33.63	0.89	37.79
n-hexane	20.11	0.66	30.47
Acetone	33.40	0.8	41.75
Acetic acid	31.95	1. 05	30.42
Oleic acid	54.50	0.894	60.96
Isopropanol	33.46	0.786	42.57
Epichlorohydrin	35.84	1.181	30.35
Diethylether	21.93	0.713	30.76
Petroleum ether	23.86	0.65	36.71
Toluene	31.80	0.87	36.55
DMF	34.90	0.948	36.81

It can be seen from Table S2 that the pore volumes were calculated based on the sorption capacity for organic liquids and their densities. The as-obtained values range from 30.35 to 85.78 cm^3 g^{-1}, which is consistent with pore volumes of *ca.* 79.31 cm^3 g^{-1} calculated from apparent density, but far from that suggested by nitrogen sorption (pore volume of 0.25 cm^3 g^{-1}). The main reason for this difference is that nitrogen sorption measurements are mainly suitable to test pores with a size between 0.35 nm and 400 nm, which do not allow for quantitative measurement of micrometer-scale pores.

Table S3. Fitting parameters of sorption kinetics of four organic liquids

Organic liquids	K (s^{-1})	Q_m (%)
Ethanol	0.932×10^{-2}	2813.6
Phenoxin	1.654×10^{-2}	6893.8
Diesel oil	1.973×10^{-4}	3314.7
Colza oil	5.291×10^{-4}	4123.4

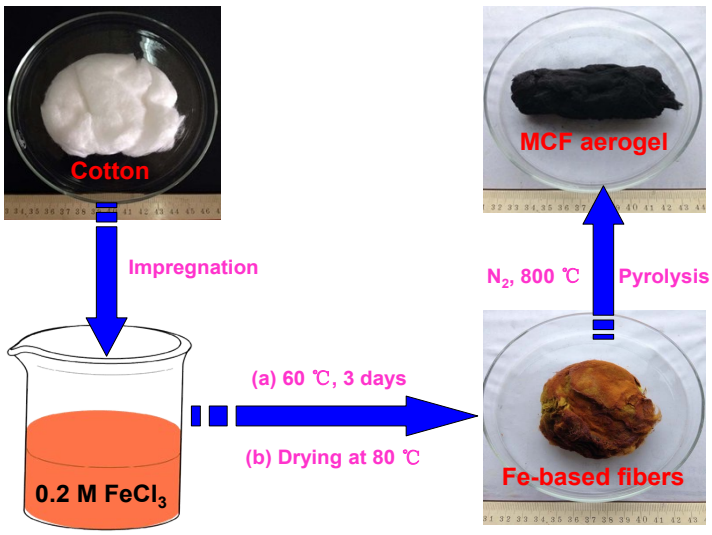

Figure S1. Illustration of the fabrication of MCF aerogel from raw cotton

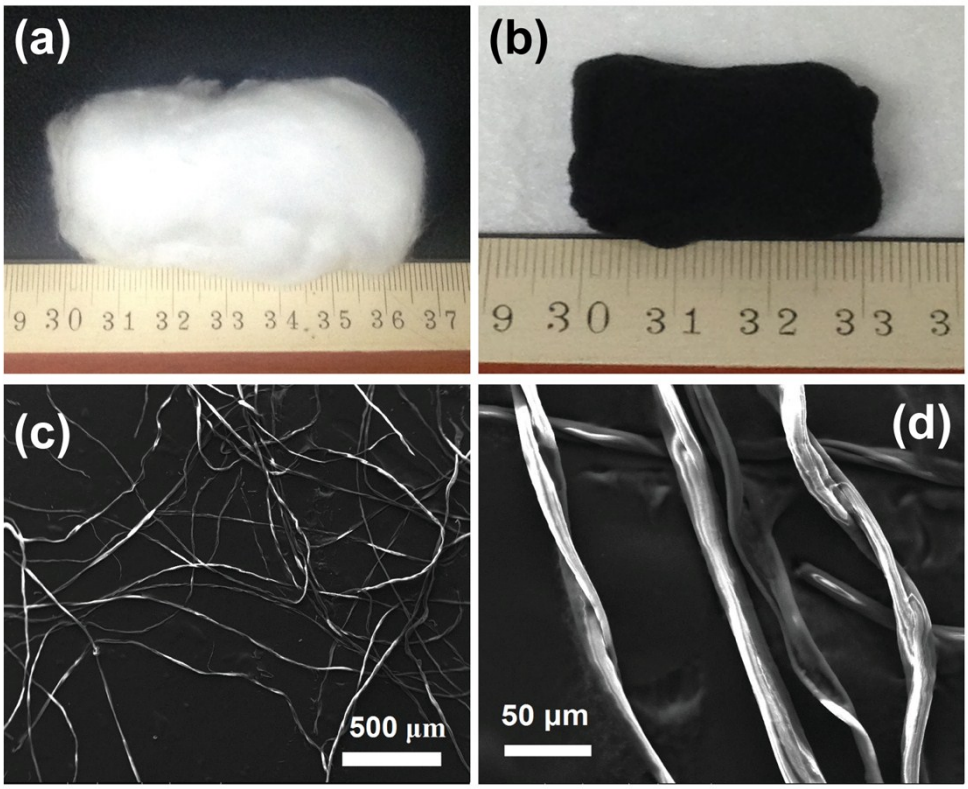

Figure S2. (a) Photograph of a piece of raw cotton, (b) photograph of a piece of MCF aerogel, (c) low-magnificaton SEM image of raw cotton fibers, (d) high magnification SEM images of cotton fibers with diameter of 20-30 μm.

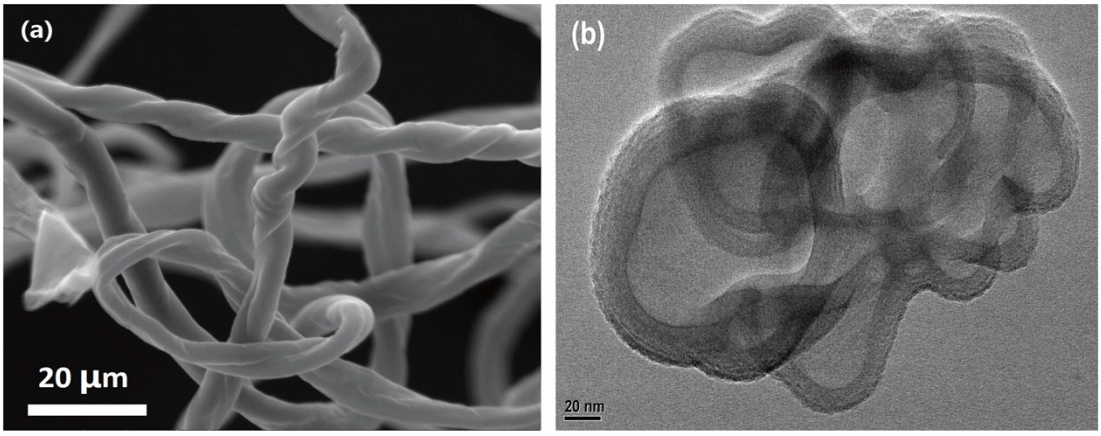

Figure S3. SEM (a) and TEM (b) images of DCC aerogel, respectively.

Figure S4. Photograph of a piece of cotton after absorption of two drop of water stained with methylene blue

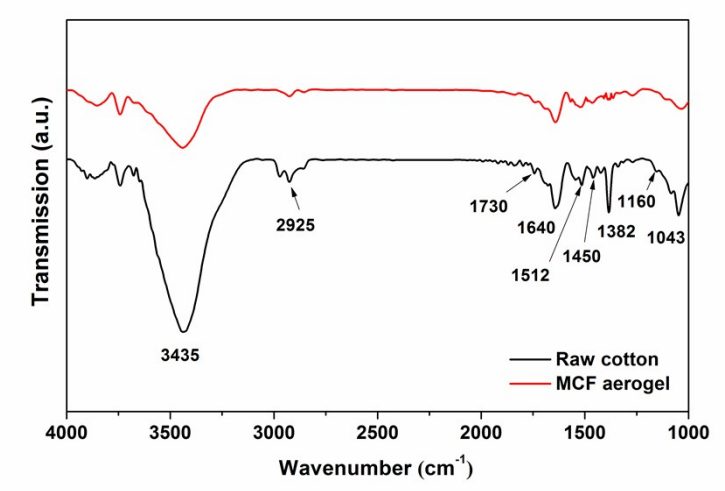

Figure S5. FTIR spectra of raw cotton and MCF aerogel

The spectrum of raw cotton shows the presence of plenty of oxygen-containing functional groups, revealed by the strong and broad peaks around 3435 cm^{-1} ascribed to hydroxyl groups, the peak at 1730 cm^{-1} attributed to carbonyl groups, and the peaks at 1087 cm^{-1} assigned to C-O bonds. The band at 1640 cm^{-1} and 1382 cm^{-1} are associated with the aromatic C-C stretching vibration of graphitic domains and COO^- groups accordingly [26, 27]. The thermal treatment of Fe-based cotton fibers resulted in a drastic decrease or disappearance of the peaks assigned to these oxide groups on raw cotton, indicating that most oxygen-containing functional groups were further removed.

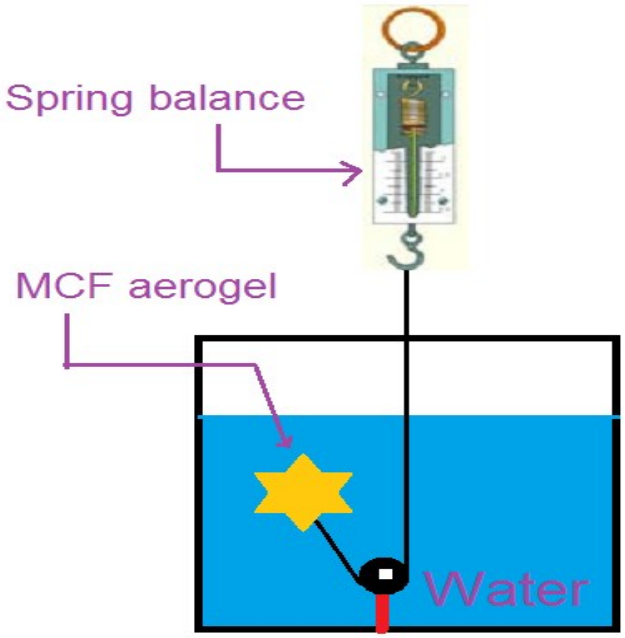

Figure S6. Schematic measuring process of the density of MCF aerogel upon Archimedes' principle

The density of MCF aerogel can be tested according to the following experimental details. Specifically, we firstly measured the mass of MCF aerogel (denoted as m_{MCF}, mg), and then conducted the experiment as shown in Figure S5 to acquire the tension (denoted as F_1, mN). Upon Archimedes' principle, the following equation should be established:

$$G_{MCF} + F_1 = F_f$$

$$G_{MCF} = m_{MCF} \times g = \rho_{MCF} \times V_{MCF} \times g$$

$$F_f = m_{water} \times g = \rho_{water} \times V_{water} \times g$$

$$V_{MCF} = V_{water}$$

Where G_{MCF} was the gravity of MCF aerogel (mN), F_1 was the tension read from the spring balance (mN), F_f was the buoyancy of MCF aerogel (mN), g was the acceleration of gravity (g/mN), m_{MCF} was the mass of MCF aerogel (mg), ρ_{MCF} was the density of MCF aerogel (mg/cm^{-3}), V_{MCF} was the volume of MCF aerogel (cm^{-3}), m_{water} was the mass of displaced water (mg), V_{water} was the volume of the displaced water (cm^{-3}).

After calculation, ρ_{MCF} can be acquired from the following equation.

$$\rho_{MCF} = (m_{MCF} \times \rho_{water} \times g)/(m_{MCF} \times g + F_1)$$

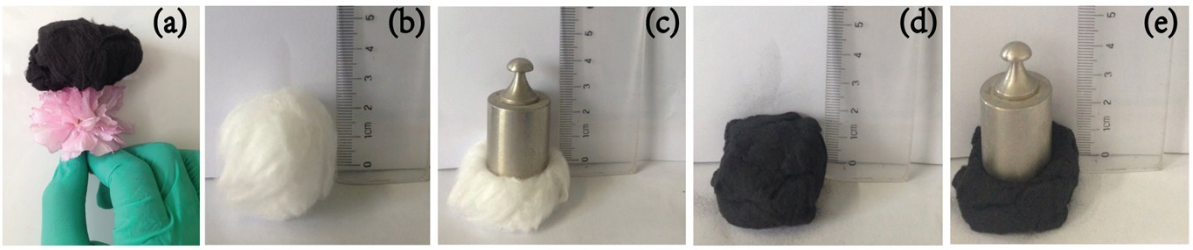

Figure S7. (a) A piece of the ultralight MCF can be placed on top of a flower, (b and c) photographs of a piece of raw cotton (left, b) before and (right, c) after a weight with weight of 100 g was placed on its top, (d and e) photographs of a piece of MCF aerogel (left, d) before and (right, e) after a weight with weight of 100 g was placed on its top.

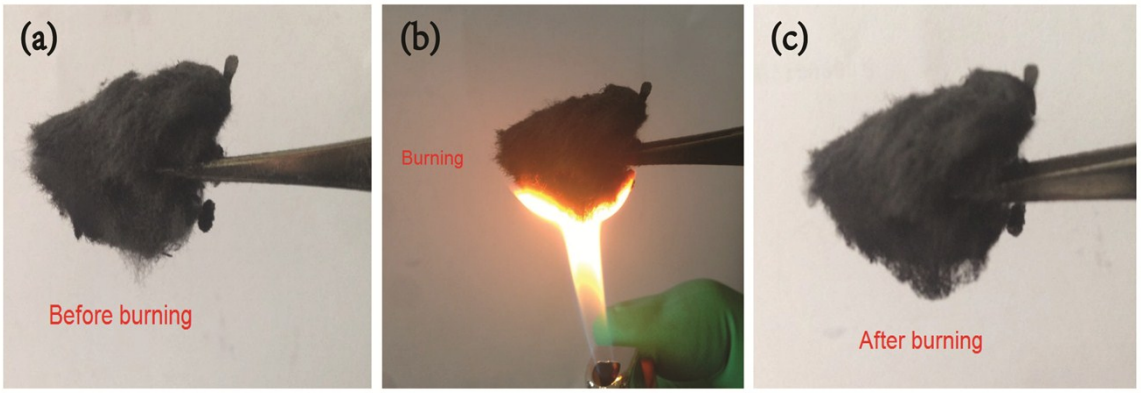

Figure S8. (a-c) Photographs of the burning process of a MCF aerogel using a lighter

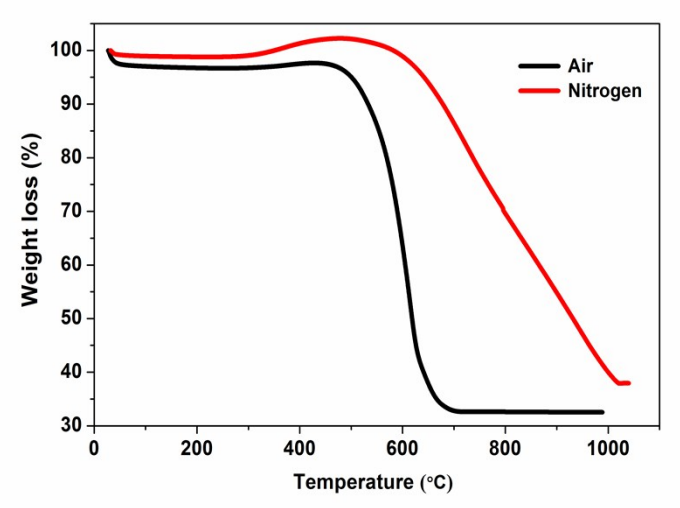

Figure S9. TG curves of MCF aerogel conducted under an air and nitrogen atmosphere accordingly.

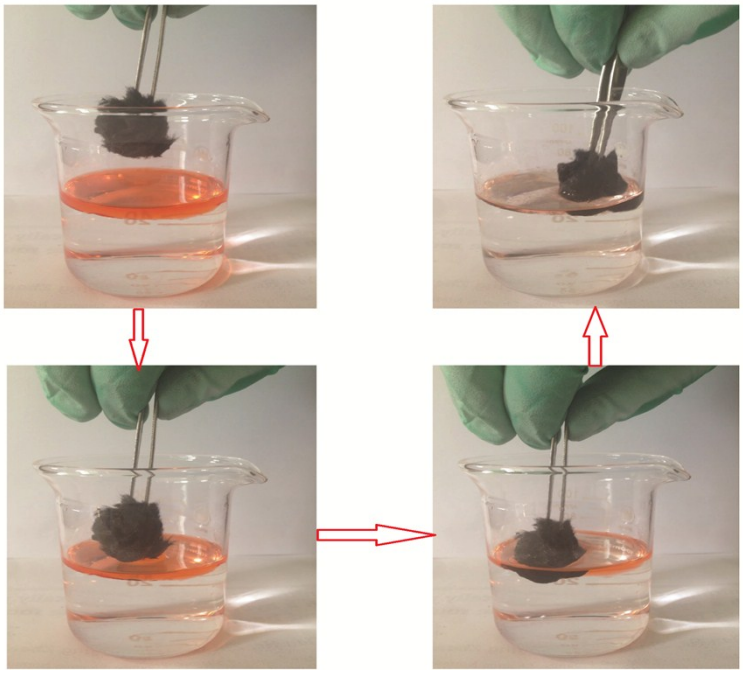

Figure S10. Photographs showing the sorption process of *n*-hexane by using a MCF aerogel taken at intervals of 10 s. *n*-Hexane stained with Sudan III floating on water was completely absorbed within 30 s.

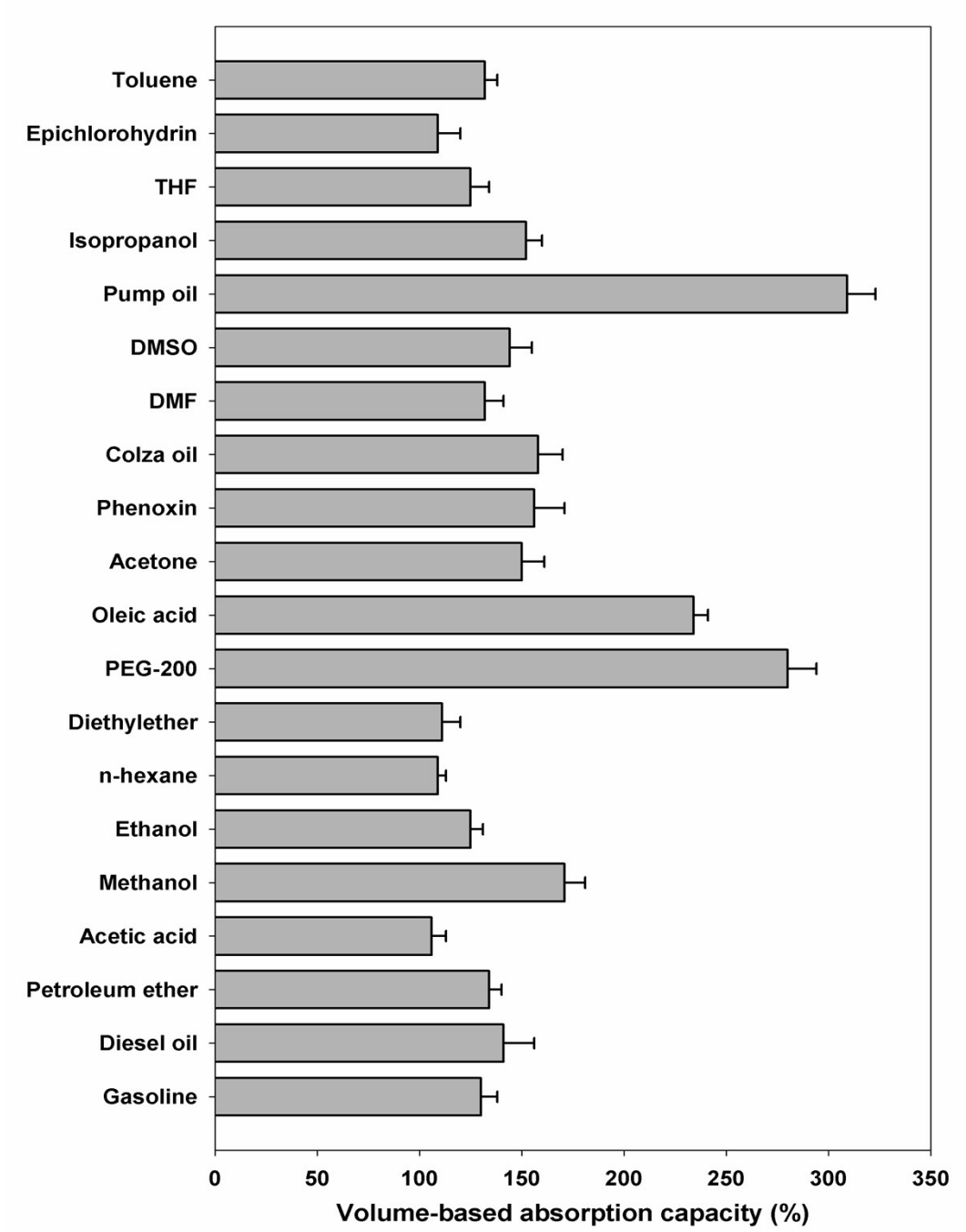

Figure S11. Sorption efficiency of the MCF aerogel for various organic liquids by volume-based absorption capacity method

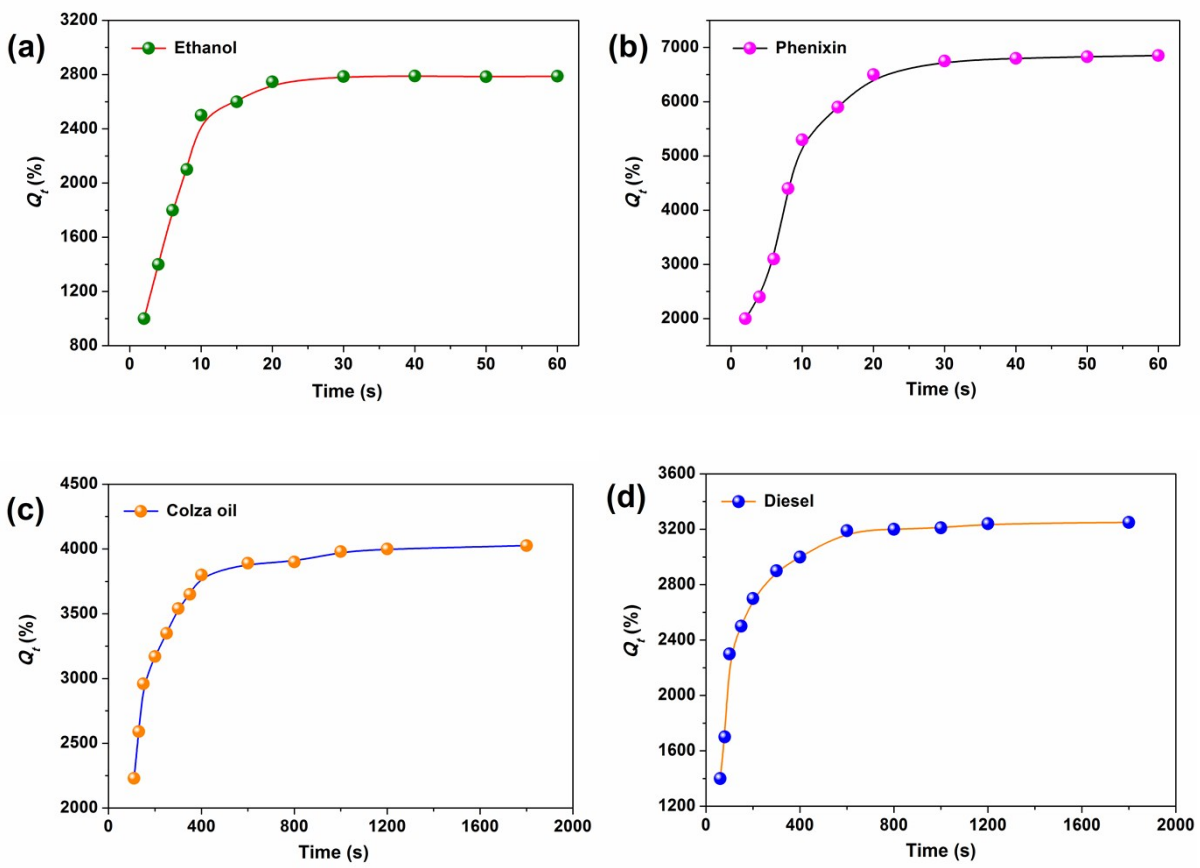

Figure S12. Sorption kinetics of four organic liquids: (a) ethanol, (b) phenoxin, (c) colza oil, and (d) diesel oil.

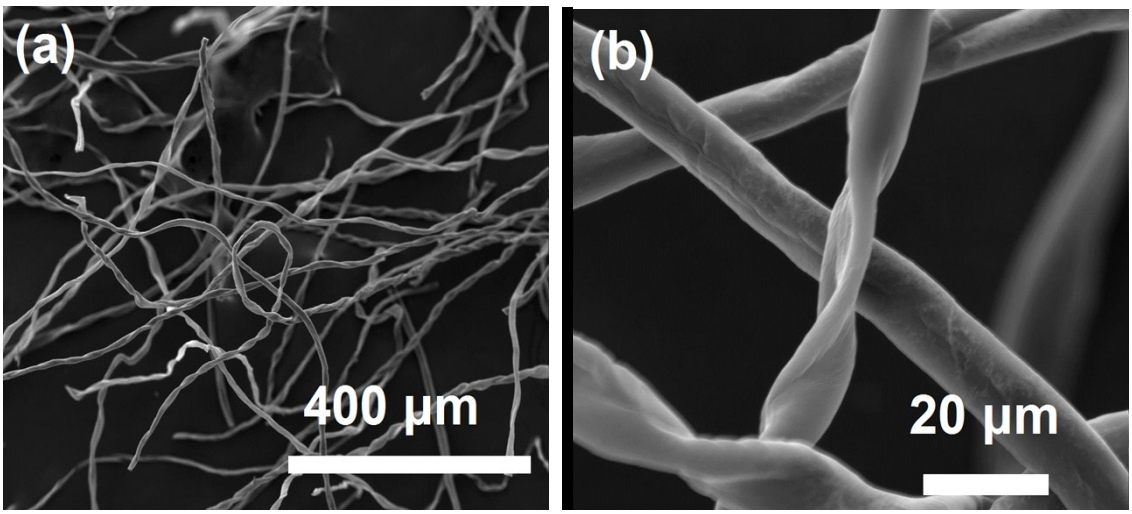

Figure S13. (a) Low- and (b) high-magnification SEM images of MCF aerogel after 5-time sorption-distillation process (Fig. 8b)

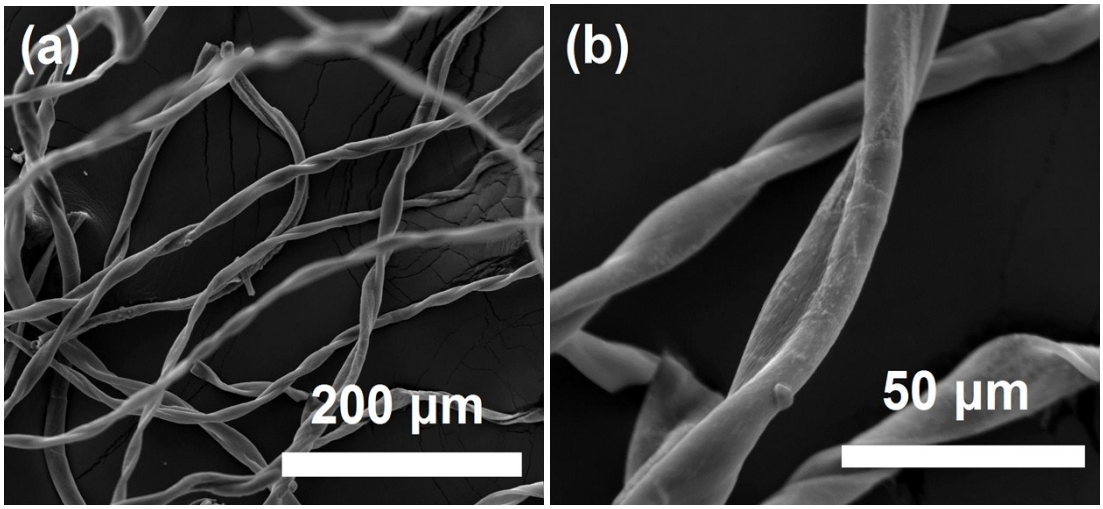

Figure S14. (a) Low- and (b) high-magnification SEM images of MCF aerogel after being recycled for 5-time sorption-combustion process (Fig. 8c). Residue particles were observed on the fiber surface.

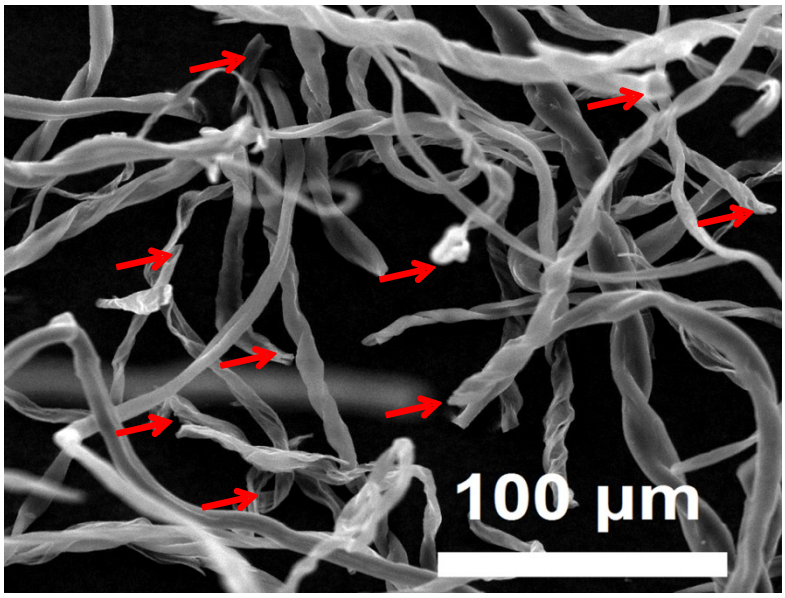

Figure S15. Low magnification SEM images of the MCF aerogel after being compressed at a strain larger than 80 %. The long fibers broke into many short segments after squeezing. The ends of broken fibers were indicated by the red arrows.

References

[1] Radetic MM, Jocic DM, Jovanccic PM, Petrovic ZL, Thomas HF. Recycled wool-based nonwoven material as an oil sorbent. Environ Sci Technol 2003; 37: 1008-1012.

[2] Annunciado TR, Sydenstricker THD, Amico SC. Experimental investigation of various vegetable fibers as sorbent materials for oil spills. Mar Pollut Bull 2005; 50: 1340-1346.

[3] Li A, Sun HS, Tan DZ, Fan WJ, Wen SH, Qing XJ, et al. Superhydrophobic conjugated microporous polymers for separation and adsorption. Energy Environ. Sci. 2011; 4: 2062-2065.

[4] Yuan J, Liu X, Akbulut O, Hu J, Suib SL, Kong J, et al. Superwetting nanowire membranes for selective absorption. Nat Nanotechnol 2008; 3: 332-336.

[5] Toyoda M, Inagaki M. Heavy oil sorption using exfoliated graphite new application of exfoliated graphite to protect heavy oil pollution. Carbon 2000 ; 38: 199-210.

[6] Lillo-Ródenas MA, Cazorla-Amorós D, Linares-Solano A. Behaviour of activated carbons with different pore size distributions and surface oxygen groups for benzene and toluene adsorption at low concentrations. Carbon 2005; 43: 1758-1767.

[7] Gui XC, Wei JQ, Wang KL, Cao AY, Zhu HW, Jia Y, et al. Carbon nanotube sponges. Adv Mater 2010; 22: 617-621.

[8] Wang G, Sun Q, Zhang Y, Fan J, Ma L. Sorption and regeneration of magnetic exfoliated graphite as a new sorbent for oil pollution. Desalination 2010; 263:183-188.

[9] Cong HP, Ren XC, Wang P, Yu SH. Macroscopic multifunctional graphene hydrogels and aerogels by metal ion induced self-assembly process. ACS Nano 2012; 6: 2693-2703.

[10] Dong XC, Chen J, Ma YW, Wang J, Chan-Park MB, Liu XM, et al. Superhydrophobic and superoleophilic hybrid foam of graphene and carbon nanotube for selective removal of oils or organic solvents from the surface of water. Chem. Commun. 2012; 48: 10660-10662.

[11] Nguyen DD, Tai NH, Lee SB, Kuo WS. Superhydrophobic and superoleophilic properties of graphene-based sponges fabricated using a facile dip coating method. Energy Environ. Sci. 2012; 5: 7908-7912.

[12] Liang HW, Guan QF, Chen LF, Zhu Z, Zhang WJ, Yu SH. Macroscopic-scale template synthesis of robust carbonaceous nanofiber hydrogels and aerogels and their applications. Angew. Chem. Int. Ed. 2012; 51, 5101-5105.

[13] Zhao J, Ren W, Cheng HM. Graphene sponge for efficient and repeatable adsorption and desorption of water contaminations. J. Mater. Chem. 2012; 22, 20197-20202.

[14] Niu Z, Chen J, Hng HH, Ma J, Chen X. A leavening strategy toprepare reduced graphene

oxide foams. Adv. Mater. 2012, 24, 4144-4150.

[15] Zhao Y, Hu C, Hu Y, Cheng H, Shi G, Qu L. A versatile, ultralight, nitrogen-doped graphene framework. Angew Chem Int Ed 2012; 51: 11371-11375.

[16] Hayase G, Kanamori K, Fukuchi M, Kaji H, Nakanishi K. Facile synthesis of marshmallow-like macroporous gels usable under harsh conditions for the separation of oil and water. Angew Chem Int Ed 2013; 52: 1986-1989.

[17] Hashim DP, Narayanan NT, Romo-Herrera JM, Cullen DA, Hahm MG, Lezzi P, et al. Covalently bonded three dimensional carbon nanotube solids via boron induced nanojunctions. Sci. Rep. 2012; 2: 363.

[18] Sun HY, Xu Z, Gao C. Multifunctional, ultra-flyweight, synergistically assembled carbon aerogels. Adv. Mater. 2013; 25: 2554-2560.

[19] Wu ZY, Li C, Liang HW, Chen JF, Yu SH. Ultralight, flexible and fire-resistant carbon nanofiber aerogels from bacterial cellulose. Angew. Chem. Int. Ed. 2013; 52: 2925-2929.

[20] Bi H, Yin Z, Cao X, Xie X, Tan C, Huang X, et al. Carbon fiber aerogel made from raw cotton: a novel, efficient and recyclable sorbent for oils and organic solvents. Adv Mater 2013; 25: 5916-5921.

[21] Chen N, Pan Q. Versatile fabrication of ultralight magnetic foams and application for oil-water separation. ACS Nano 2013; 7(8): 6875-6883.

[22] Chu Y, Pan Q. Three-dimensionally macroporous Fe/C nanocomposites as highly selective oil-absorption materials. ACS Appl. Mater. Interfaces 2012; 4: 2420-2425.

[23] Juuso TK, Marjo K, Robin HAR, Olli I. Hydrophobic nanocellulose aerogels as floating, sustainable, reusable, and recyclable oil absorbents. ACS Appl. Mater. Interfaces 2011; 3: 1813-1816.

[24] Bi H, Xie X, Yin K, Zhou Y, Wan S, He L, et al. Spongy graphene as a highly efficient and recyclable sorbent for oils and organic solvents. Adv. Funct. Mater. 2012; 22: 4421-4425.

[25] Li Y.-Q, Samad YA, Polychronopoulou K, Alhassan SM, Liao K. Carbon aerogel from winter melon for highly efficient and recyclable oils and organic solvents absorption. ACS Sustainable Chem. Eng. 2014; *2* (6): 1492-1497.

[26] Socrates G. Infrared characteristic group frequencies; tables and charts, 2nd ed., John Wiley & Sons, 1994**.**

[27] Liu R-L, Ji W-J, He T, Zhang Z-Q, Zhang J, Dang F-Q. Fabrication of nitrogen-doped hierarchically porous carbons through a hybrid dual-template route for CO_2 capture and haemoperfusion. Carbon, 2014, 76: 84-95.